Scientific
Research
Publishing

In Silico Modeling of C1 Metabolism

Santhiya Kothandaram, Prabhakar Deonikar, Mrudhuula Mohan, Vyshali Venugopal, V. A. Shiva Ayyadurai*

Systems Biology Group, International Center for Integrative Systems, Cambridge, MA, USA
Email: *vashiva@integrativesystems.org

Abstract

An integrative computational, *in silico*, model of C1 metabolism is developed from molecular pathway systems identified from a recent, comprehensive systematic bioinformatics review of C1 metabolism. C1 metabolism is essential for all organisms to provide one-carbon units for methylation and other types of modifications, as well as for nucleic acid, amino acid, and other biomolecule syntheses. C1 metabolism consists of three important molecular pathway systems: 1) methionine biosynthesis, 2) methylation cycle, and 3) formaldehyde detoxification. Each of the three molecular pathway systems is individually modeled using the CytoSolve® Collaboratory™, a proven and scalable computational systems biology platform for *in silico* modeling of complex molecular pathway systems. The individual models predict the temporal behavior of formaldehyde, formate, sarcosine, glutathione (GSH), and many other key biomolecules involved in C1 metabolism, which may be hard to measure experimentally. The individual models are then coupled and integrated dynamically using CytoSolve to produce, to the authors' knowledge, the first comprehensive computational model of C1 metabolism. *In silico* modeling of the individual and integrated C1 metabolism models enables the identification of the most sensitive parameters involved in the detoxification of formaldehyde. This integrative model of C1 metabolism, giving its systems-based nature, can likely serve as a platform for: 1) generalized research and study of C1 metabolism, 2) hypothesis generation that motivates focused and specific *in vitro* and *in vivo* testing in perhaps a more efficient manner, 3) expanding a systems biology understanding of plant bio-molecular systems by integrating other known molecular pathway systems associated with C1 metabolism, and 4) exploring and testing the potential effects of exogenous inputs on the C1 metabolism system.

Keywords

---

*Corresponding author.

1. Introduction

C1 metabolism is one of the most important biological processes in living systems responsible for providing one-carbon units for proteins, nucleic acids, methylated compounds, and other biomolecules. The C1 metabolism system is mostly found in plants, bacteria, fungi, and mammals [1] [2]. A wide variety of important biomolecules are synthesized in C1 metabolism such as methionine, formylmethionine-tRNA, pantothenate, thymidylate, adenosine, and serine. More importantly, the C1 metabolism process provides the one-carbon units essential for DNA methylation, which controls plant growth and development, with a particular involvement in regulation of gene expression and DNA replication [3].

This research presents, to the authors' knowledge, the first computational, *in silico*, model of C1 metabolism. The significance of this model, giving its systems-based nature, is that it can likely serve as a platform for: 1) generalized research and study of C1 metabolism, 2) hypothesis generation that directs more focused and specific *in vitro* and *in vivo* testing, in a more efficient manner, 3) expanding a systems biology understanding of plant bio-molecular systems by integrating other known molecular pathway systems associated with C1 metabolism, and 4) exploring and testing the potential effects of exogenous inputs on the C1 metabolism system.

This model is based on an earlier systematic review of literature [4] that resulted in the identification of three critical molecular pathway systems of C1 metabolism: 1) methionine biosynthesis, 2) activated methyl cycle, and 3) formaldehyde detoxification. Two major insights emerged from this earlier systematic review. The first major insight is that while C1 metabolism normally proceeds from serine to methionine where a carbon group is donated to a biomolecule in a methylation reaction, in photosynthetic tissues, however, C1 metabolism appears to proceed in reverse, synthesizing serine and oxidizing formate. The second major insight is that formaldehyde detoxification pathway can be blocked by a modification to s-formylglutathione hydrolase, which may cause the accumulation of formaldehyde if there is no alternative detoxification path. This earlier work provides the foundation for enabling the development of a predictive and integrative computational model, *in silico* model, of C1 metabolism based on the extant literature.

In this paper, the CytoSolve® Collaboratory™, a proven and scalable computational systems biology approach [5], is employed to convert the diagrammatic representations of the three molecular pathway systems of C1 metabolism, identified from the earlier systematic review [4], into three individual molecular pathway models. The three molecular pathway models are then coupled dynamically using CytoSolve to produce an integrative computational model of C1 metabolism.

The CytoSolve platform performs such integration by abstracting complex cellular functions as a plurality of molecular pathways, each of which can be treated as individual molecular pathway models, as shown in **Figure 1**, spanning multiple spatial and temporal scales, across compartments, cell types and biological domains [5] [6]. This approach allows for an inherent scalability to build models of complex biological phenomena, not afforded by other known methods, since CytoSolve obviates the need to create one large monolithic model [6], which can be neither modularly scaled nor maintained, giving the dynamic nature of biological research.

The resulting integrative model of C1 metabolism provides an *in silico* method to gain systems-level understanding of complex cellular functions not possible through conventional *in vitro* and *in vivo* approaches. The C1 metabolism modeling, for example, predicts the temporal behavior of formaldehyde, formate, sarcosine, glutathione (GSH), as well as many other key biomolecules involved in C1 metabolism, which may be hard to measure experimentally.

1.1. C1 Metabolism

C1 metabolism is essential for all organisms to provide one-carbon units for methylation and other types of modifications, as well as for nucleic acid, amino acid, and other biomolecule syntheses. In particular, C1 metabolism process provides the one-carbon units essential for DNA methylation, which controls plant growth and development, with a particular involvement in regulation of gene expression and DNA replication [3].

DNA methylation in plants, similar to that in animals, affects the ability of specific proteins to bind to the DNA and chromatin based transcription complex formation, and also related to histone modifications. Methylation in plants is species-, tissue-, organelle- and age-specific. In plants, DNA is highly methylated; containing 5-methylcytosine (m5C) and N 6-methyladenine (m6A) [3].

C1 metabolism in plants, however, differs in fundamental ways from that in bacteria, fungi, and mammals. In plants, one carbon transfer is very critical for plant specific metabolic pathways such as photorespiration, mitochondrial formate metabolism, glyoxylate metabolism, and the methylation cycle.
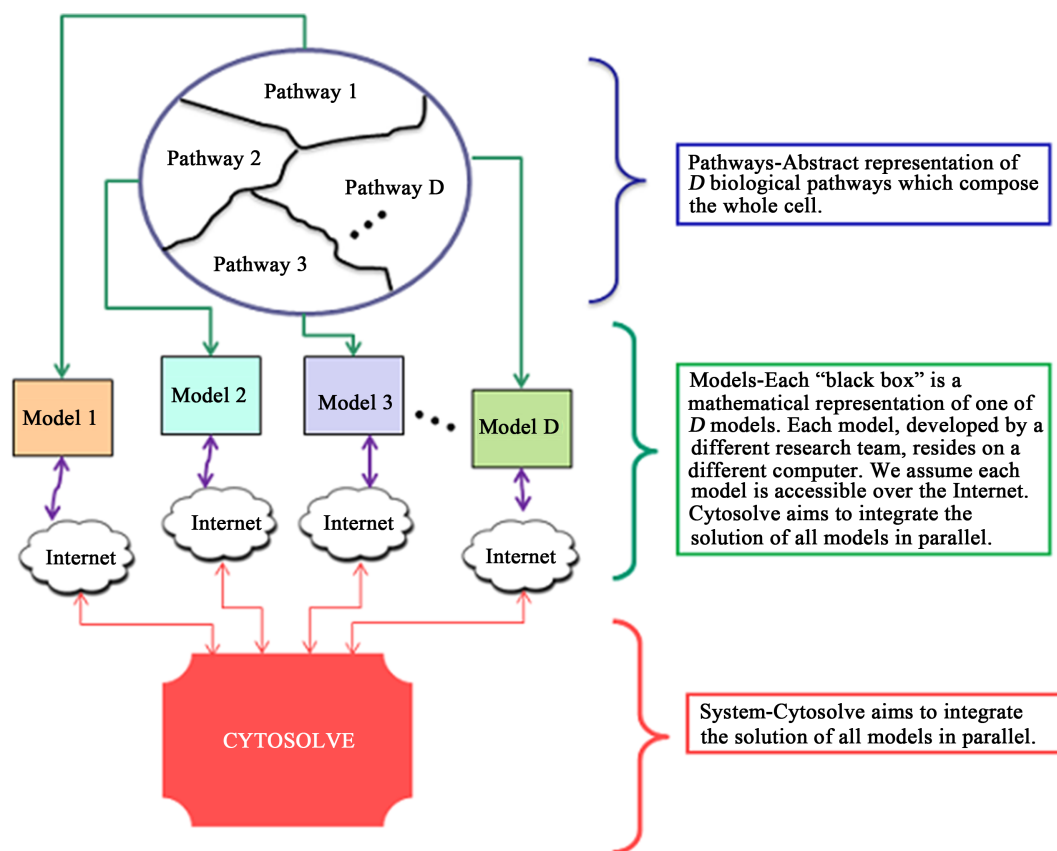
Figure 1. CytoSolve provides a framework for integrating systems of systems of molecular pathway models [5] [6].

Perturbations to C1 metabolism, therefore, may likely affect the control mechanisms of DNA methylation, which itself is modulated by phytohormones and changes on seed germination, flowering and under the influence of various pathogens (viral, bacterial, fungal). At the enzymatic level, the common enzymes that plants share with other organisms have been shown to have different roles in plants. Formaldehyde dehydrogenase and s-formylglutathione hydrolase, for example, are known to metabolize endogenous formaldehyde and not exogenous formaldehyde from the environment [2].

C1 metabolism is a complex system of molecular pathway systems. The three major molecular pathway systems of C1 metabolism, aforementioned, are summarized from the previous systematic literature review to provide the reader a background to appreciate the *in silico* modeling efforts herein.

1.2. Methionine Biosynthesis

One of the three systems of C1 metabolism is *methionine biosynthesis*. Methionine biosynthesis is comprised of set of reactions that are folate-dependent as shown in **Figure 2** [4]. The starting point for methionine synthesis is the addition of either serine [7] or the formate molecule [8] to tetrahydrofolate (THF), followed by several interconversions that lead to methionine biosynthesis [9]. Formate can also get oxidized to carbon dioxide (CO_2) or dimerize to yield glyoxylate [10]. The last step in this set of molecular pathways is the synthesis of methionine. Reaction between homocysteine and a THF derivative catalyzed by methionine synthase leads to the formation of methionine in either the cytosol or chloroplast [11].

The major vehicles of one carbon unit transfer are various complexes of THF present mostly in cytosol [12]-[14], as well as the mitochondria and chloroplast [15]. The synthesis of THF spans the chloroplast, cytosol, and mitochondrion. The precursor of THF, dihydropterin, is synthesized in cytosol whereas p-aminobenzoic acid is synthesized in chloroplast. They are translocated into the mitrochondrion for completion of THF synthesis [16] [17].
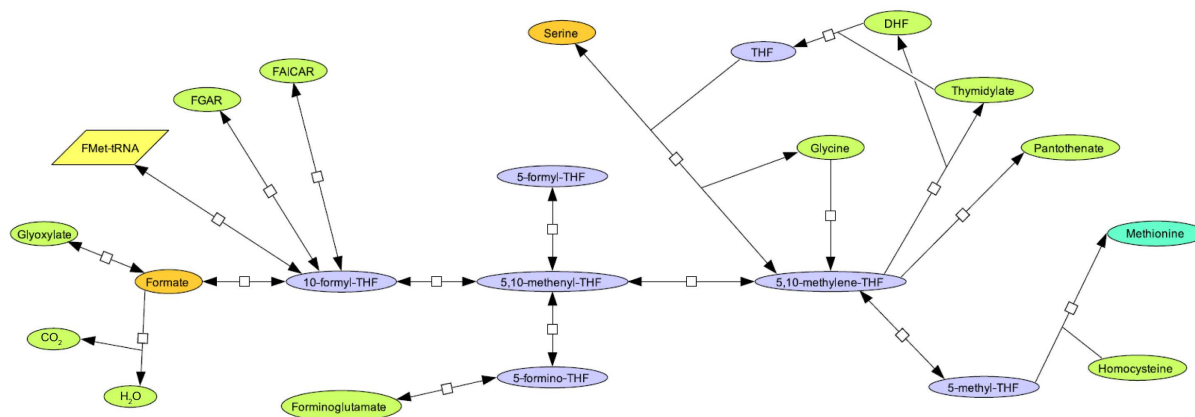
Figure 2. Methionine biosynthesis. Interconversion of folate derivatives (in blue) results in methionine biosynthesis. Abbreviations: formylmethionine tRNA (FMet-tRNA); formylglycinamide ribonucleotide (FGAR); formamidoimidazolecarboxamide ribonucleotide (FAICAR); dihydrofolate (DHF) [4].

1.3. Activated Methyl Cycle

Another important system of C1 metabolism is the *activated methyl cycle*, as shown in **Figure 3**. Of the total methionine synthesized from the methionine biosynthesis pathway, 20% is utilized for protein synthesis [18]. The remaining methionine may be the used in theactivated methyl cycle.

Methionine in the activated methyl cycle is converted to S-adenosylmethionine (SAM) in the cytosol [11] [19]-[21] and can be translocated to chloroplast for methylation [11]. Methyltransferase enzymes bind to SAM, which binds to enzymes [22] to form a complex. This SAM-bound enzymes subsequently transfers the methyl group to methylate DNA, RNA, proteins, and other biomolecules to complete the methylation process. Loss of methyl group from SAM yields s-adenosylhomo-cysteine which dissociates into adenosine and homocysteine [23]. Homocysteine is then converted back to methionine [23] and recycled.

1.4. Formaldehyde Detoxification

Within C1 metabolism, *formaldehyde detoxification* as shown in **Figure 4**, is a critical system for modulating formaldehyde levels. Formaldehyde is a toxic compound produced during plant C1 metabolism. The detoxification of formaldehyde therefore is essential to normal cellular function in plants.

The main sources of formaldehyde in plants are 5, 10-methylene-THF, methanol, and sarcosine [24] [25]. The detoxification of formaldehyde results in either formate or a THF derivative [4]. Formate can either be further oxidized to CO_2 [26] or utilized as a carbon source in C1 metabolism.

In this process, formaldehyde may bind to either to glutathione (to form hydroxylmethylglutathione (HM-glutathione)) [27] or to a THF derivative. Conversion of HM-glutathioneto formate involves its catalysis by formaldehyde dehydrogenase (FALDH) to formylglutathione (formyl-GSH). In the final steps, formylglutathione is converted to formate and glutathione which is catalyzed by s-formylglutathione hydrolase [28]-[31].

2. Methods

Computational systems biology approaches can provide insights to understand complex molecular phenomena. In this research, the CytoSolve technology and methodology are applied to develop an integrative and predictive computational model of C1 metabolism. The CytoSolve technology and approach involves a six-step process to produce such an integrative model [6]. The steps are as follows:

1. Conduct and archive search results of scientific literature from disparate data sources including PubMed, Google Scholar, and multiple online databases;

2. Identify molecular pathway diagrams from the extant literature, while annotating, archiving, and managing the sourced literature for subsequent review and access;

3. Review the identified molecular pathway diagrams to construct a cogent *systems architecture* that provides a blueprint for future *in silico* modeling the of the molecular system of interest;
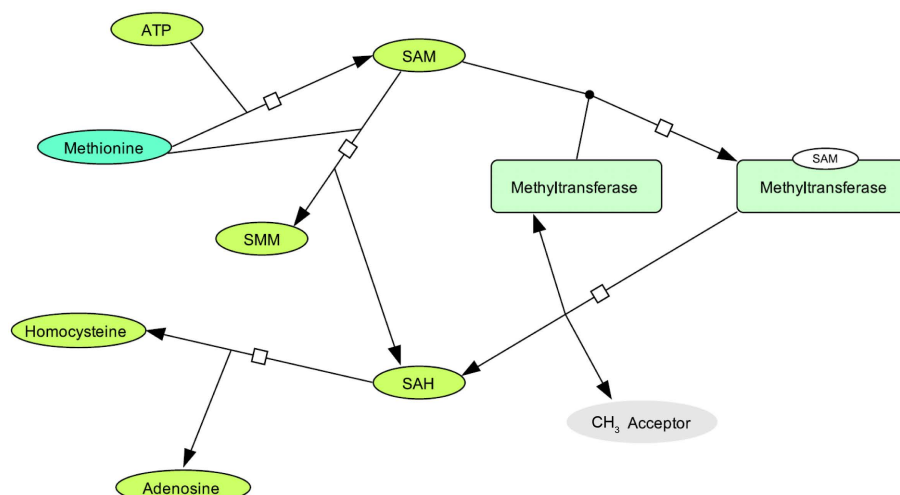
Figure 3. Activated methyl cycle. A one-carbon molecule is passed from methionine to a methyl group acceptor catalyzed by methyltransferase enzyme. Abbreviations: s-adenosylmethionine (SAM); s-methylmethionine (SMM); s-adenosylhomocysteine (SAH) [4].
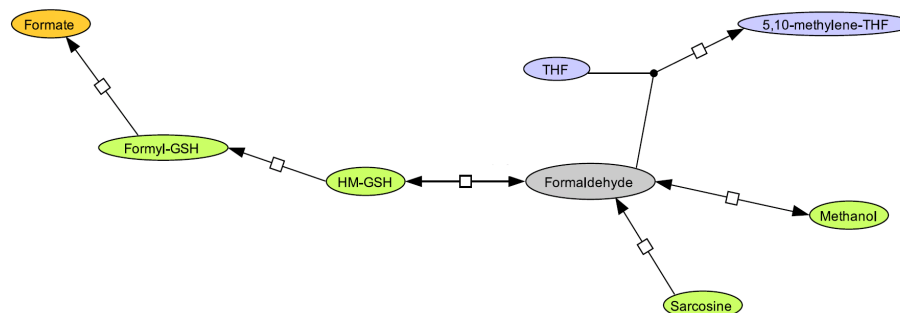
Figure 4. Formaldehyde detoxification. Formaldehyde is detoxified into formate through a series of intermediaries including: s-hydroxymethylglutathione (HM-GSH), formylglutathione (formyl-GSH) [4].

4. Identify critical modelling parameters such as rate constants and initial conditions, to enable the conversion of the diagrammatic molecular pathway representations to predictive mathematical models;

5. Create and simulate component (individual) molecular pathway models; and,

6. Integrate and couple the component models to create a dynamic, scalable and predictive model of the biological phenomena of interest.

In this effort, since Steps (1-2) were completed in the earlier work [4], the *in silico* modeling process of this research begins with Step 3.

2.1. CytoSolve Background

CytoSolve, developed in earlier work by Ayyadurai and Dewey (2011) [5], provides a scalable computational systems biology platform for the dynamic integration of complex and large-scale molecular pathway models [5] [6] [32]. CytoSolve was selected for use in this research since, it allows for complex and scalable integration of multiple molecular pathway models.

CytoSolve aggregates existing peer-reviewed scientific literature and mines this literature to extract molecular pathways of biological processes. Mathematical models derived from these pathways are integrated to create a validated and integrative model. This method provides a computational architecture, as shown in **Figure 5**, for coupling individual molecular pathway models dynamically without the need to create a monolithic model.

This approach provides a scalable methodology for integration of systems of systems of molecular pathway models. Other computational approaches are not scalable as they have not considered the intractability that
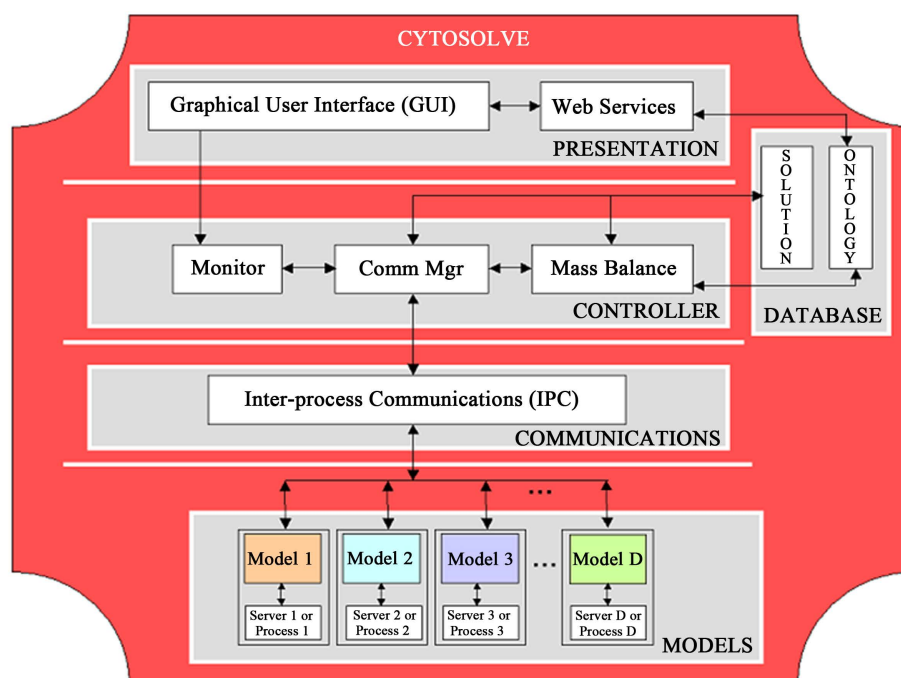
Figure 5. The CytoSolve software architecture framework for integrating systems of systems of molecular pathway models [5].

emerges from maintaining a single large monolithic model, wherein each model, within a system of molecular pathway model may require constant updates and changes, given the dynamic nature of biological research [6].

2.2. S ystems Architecture of C1 Metabolism

In silico modeling benefits greatly through a high level architecture, which provides a blueprint on how the elemental pathway systems integrate as well as an understanding of how such systems may interact with related systems. This effort results in the development of a *systems architecture* map. This systems architecture map provides a cogent approach not only to produce an integrative model, but also to appreciate how other related systems, in future research, can be integrated to expand more complex understanding of the phenomena of interest.

2.3. *In Silico* Modeling of Individual Molecular Pathway Systems

The CytoSolve platform enables the development of three *in silico* molecular pathway models: 1) methionine biosynthesis, 2) activated methyl cycle, and 3) formaldehyde detoxification. For each individual pathway, relevant literature is identified, reviewed and prioritized. Key reactions in the individual pathways are identified from the relevant literature along with appropriate kinetic information, as well as the biomolecular species and their concentration information.

In the *Supplementary Materials*, are provided the sources of the kinetic information used in deriving the individual molecular pathway models. **Tables S1-S3** of the Supplementary Material contain the kinetic information for methionine biosynthesis, activated methyl cycle, and formaldehyde detoxification models, respectively. The *Supplementary Materials* also provides the literature references from which the kinetics are obtained for developing the *in silico* models.

2.4. Integration of Molecular Pathway Systems to Produce a Dynamic Integrative Model

The three validated molecular pathway models of methionine biosynthesis, activated methyl cycle and formaldehyde detoxification are integrated in the CytoSolve platform to create an integrative and comprehensive *in silico* model of C1 metabolism. This integration is modular and dynamic, meaning the individual models remain

in their native formats, and intelligent computational engine afforded by CytoSolve provides a mechanism to dynamically integrate the individual models, based on identification of common biomolecular species across a plurality of a system of models. For example, in one case, the two molecular species: homocysteine and methionine are common species across the two molecular pathway systems of methionine biosynthesis and active methyl cycle models. In another example, 5,10-methylene THF and formate are the common molecular species across the molecular pathway systems of methionine biosynthesis and formaldehyde detoxification pathways.

2.5. Simulation and Verification

The integrative model resulting from the coupling of the three molecular pathway systems of C1 metabolism can be used for executing simulations through CytoSolve, which performs mass balance and simultaneously couples and solves the systems of systems of differential equations to estimate the rate curves for each biomolecular species within the C1 metabolism system to estimate the concentration profiles of biomolecules in C1 metabolism. All simulations were executed for a simulation time period of 800,000 seconds (~9 days). These simulations provide the insights for conducting *in silico* modeling and testing of biological phenomena to support *in vitro* and *in vivo* research.

3. Results

There are six sets of results, which emerge from the research herein. The first set of results, in section 3.1, is a high-level systems architecture of C1 metabolism. The next three sets of results are the simulation output from executing each of the individual *in silico* models of methionine biosynthesis, active methyl cycle and formaldehyde detoxification, in sections 3.2, 3.3 and 3.4, respectively. The fifth set of results is the simulation output from the integrative model of C1 metabolism, which offers insights based on the coupling of the three models. Finally, the sixth set of results is the sensitivity analysis to provide a detailed understanding of which parameters are critical in the modeling of C1 metabolism.

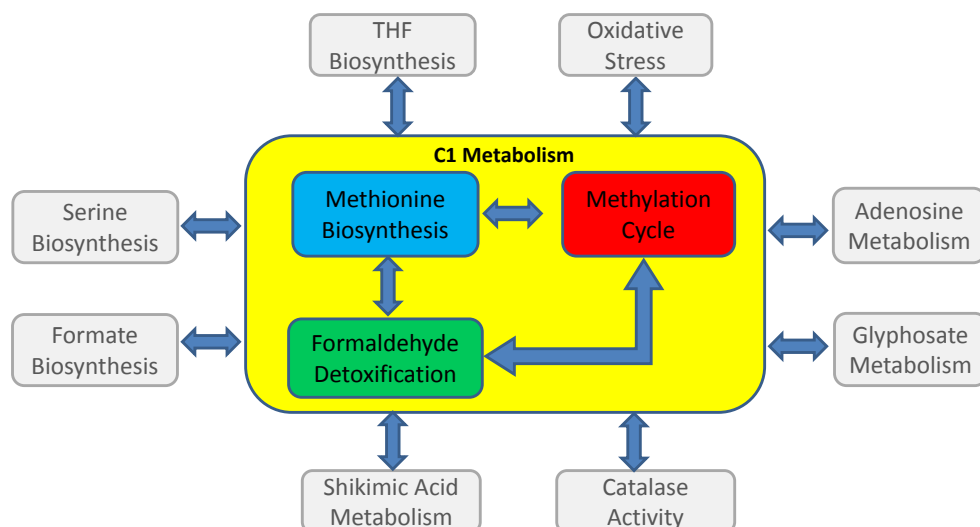### 3.1. Systems Architecture of C1 Metabolism

The systems architecture map of C1 metabolism is shown in **Figure 6**. This figure is the schematic illustration of how the three major molecular systems of methionine biosynthesis, activated methyl cycle and formaldehyde detoxification illustrated in **Figures 2-4**, respectively, interconnect and interface with one another.

The schematic illustration in **Figure 6** shows that each molecular pathway system of C1 metabolism interacts with the other two. Methionine biosynthesis, shown in **Figure 2**, communicates with formaldehyde detoxification, shown in **Figure 4**, via the common molecular specie of THF and 5,10-methylene-THF. Methionine biosynthesis communicates with activated methyl cycle, shown in **Figure 3**, via the common molecular specie of methionine and homocysteine. The activated methyl cycle communicates with formaldehyde detoxification via the common molecular species of sarcosine.

In addition to the core elements of C1 metabolism illustrated in **Figure 6**, **Figure 7** illustrates, based on the current literature review, other molecular pathway systems that may likely interact with C1 metabolism. These systems include: THF biosynthesis, oxidative stress metabolism, catalase activity, shikimic acid metabolism, adenosine metabolism, glyphosate metabolism, formate biosynthesis, and serine biosynthesis.
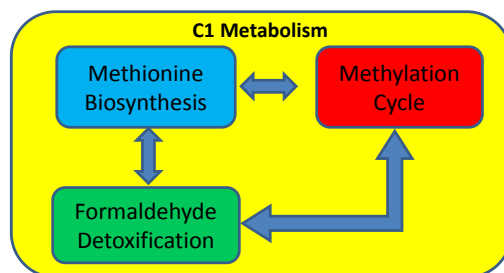
Figure 6. Systems architecture of C1 metabolism. This figure provides the schematic illustration of how methionine biosynthesis, activated methyl cycle and formaldehyde detoxification interconnect in the C1 metabolism.

Figure 7. Systems architecture for C1 metabolism interrelations with other plant pathways.

The key biomolecular species of interest in the methionine biosynthesis model are methionine and formaldehyde. The methionine biosynthesis model was simulated for a simulation time period of 800,000 seconds (~9 days). There are three important results that emerged from this simulation.

First, the model predicts that methionine concentrations reach saturation levels of 1000 nM, near instantaneously relative to the simulation time of period of 800,000 seconds (~9 days), as shown in **Figure 8(a)**. The individual model of methionine biosynthesis only considers the reaction of formation of methionine and not its consumption in downstream pathways; therefore, the methionine concentrations reacha plateau and achieve a steady state. The steady state value 1000 nM of methionine resultsfromthe complete conversion of homocysteine, which is reported to have 1000 nM in physiological conditions [33]. The results indicate that all of the homocysteine is converted to methionine in the methionine biosynthesis model.

The second result is concerning formaldehyde formation in the methionine biosynthesis model as shown in **Figure 8(b)**. Formaldehyde is produced from 5, 10-methylene THF [13] [34] in the methionine biosynthesis model. A steady state concentration of 0.06 nM of formaldehyde is achieved near instantaneously in methionine biosynthesis model.

The third result is concerning formate concentrations in the methionine biosynthesis model as shown in **Figure 8(c)**. Formate is produced from formylglutathione (formyl-GSH) and consumed in the methionine biosynthesis model [28] [35]. Formate rapidly increases as it synthesized from formylglutathione and is converted to CO_2 and water in the methionine biosynthesis model which explains the near instantaneous rise in formate concentrations followed by decrease in its concentrations with time. Since the formate concentrations are obtained from the mass balance of formate, the reduction in formate concentrations over time indicates that the conversion of formate to CO_2 is dominant relative to the formation of formate from formylglutathione.
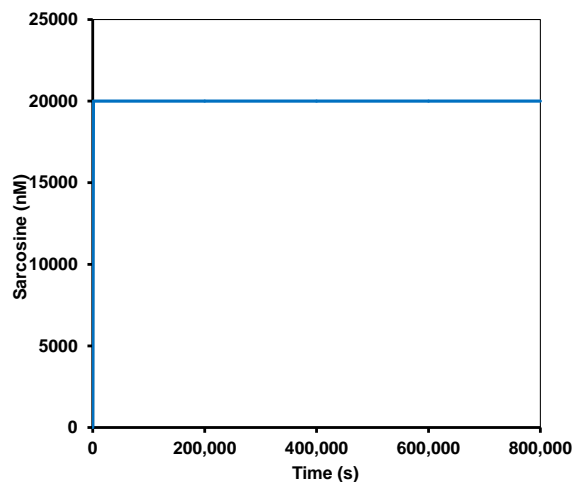
3.2. Activated Methyl Cycle Simulation Results

There is one important result that emerges from this simulation as shown in **Figure 9**. One of the key reactions in activated methyl cycle is the transfer of methyl group from glycine to an acceptor such as sarcosine [36] [37]. Since sarcosine is an important mediator in the transfer of methyl group, observing its temporal change in simulation provides us critical insights into the state of the activated methyl cycle. The activated methyl cycle model was simulated for a simulation time period of 800,000 seconds (~9 days).

The model predicts that the sarcosine concentrations reach steady state levels of 2000 nM near instantaneously. This is likely since sarcosine is synthesized and not consumed in activated methyl cycle model. Even though glycine is present in excess amounts [33], sarcosine concentration does not increase with time as there is a limited amount of methyl-group transfer from s-adenosylhomocysteine, which is required for sarcosine production.
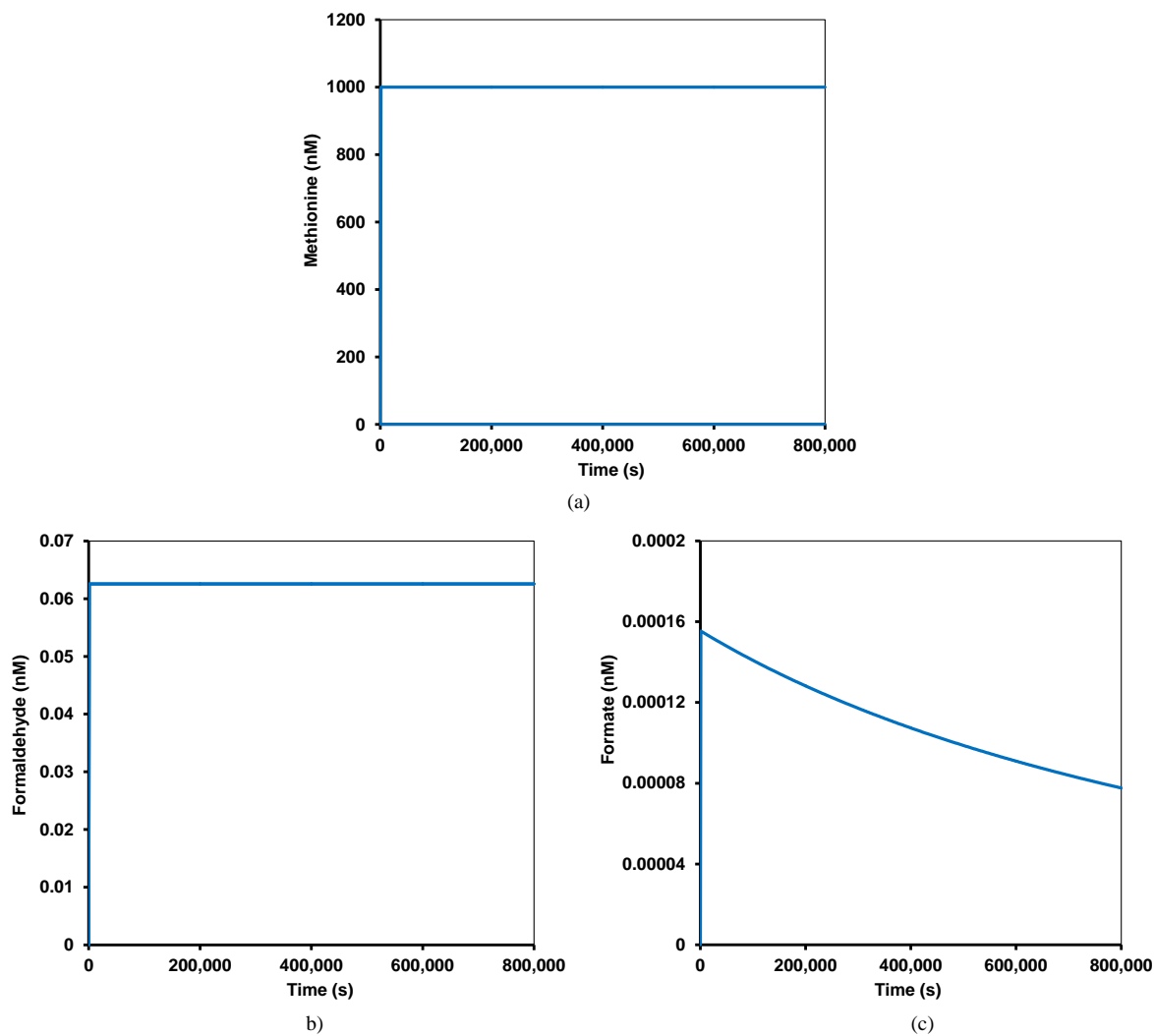
Figure 8. (a) Simulation results of methionine concentration from methionine biosynthesis model; (b) Simulation results of formaldehyde concentration from methionine biosynthesis model; (c) Simulation results of formate concentration from methionine biosynthesis model.

Figure 9. Simulation results of sarcosine concentration from activated methyl cycle model.
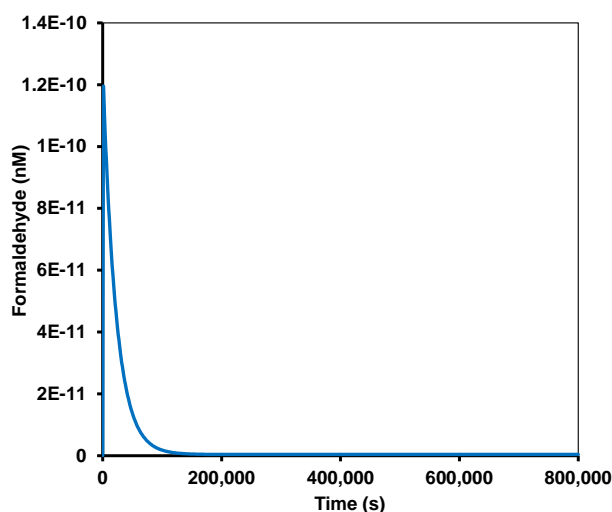
3.3. Formaldehyde Detoxification Simulation Results

Formaldehyde (HCHO), which is synthesized in the methionine biosynthesis cycle, enters the formaldehyde detoxification model where it is eventually converted to CO_2 and water (H_2O) [38]. The sources of formaldehyde synthesis include 5, 10-methylene-THF, methanol and sarcosine [24] [39] [40]. Detoxification of formaldehyde is glutathione (GSH) dependent [41]. GSH-formaldehyde adduct undergoes series of inter-conversions catalyzed by FALDH resulting in formate [28] [42]. Formate is then converted to CO_2 and water by formate dehydrogenase.
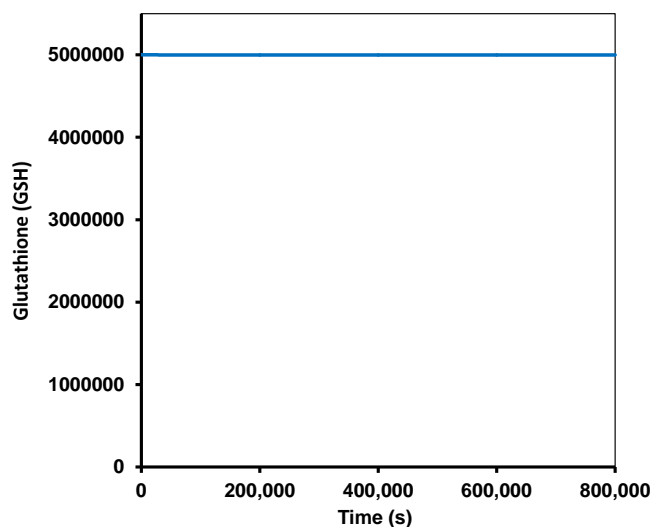
The formaldehyde detoxification model was simulated for a simulation time period of 800,000 seconds (~9 days). Two biomolecular species are of particular interest in this simulation: formaldehyde and glutathione.

As shown in **Figure 10**, formaldehyde starts initially at a low, non-zero level, and decays, detoxified, within ~120,000 seconds (~1.5 days) to zero. These results indicate that during normal plant metabolism, formaldehyde is efficiently cleared in the formaldehyde detoxification pathway.

Since glutathione (GSH), an important antioxidant, is necessary for clearance of formaldehyde in the formaldehyde detoxification pathway, simulation results of glutathione's temporal dynamics are generated. The simulation results, in **Figure 11**, indicate that during normal plant metabolism, glutathione levels are stable and static and maintain a steady state level of 5 mM.

Figure 10. Simulation results of formaldehyde concentration from formaldehyde detoxification model.

Figure 11. Simulation results of glutathione (GSH) concentration from formaldehyde detoxification model.

3.4. C1 Metabolism Model Simulation Results

The individual models representing methionine biosynthesis, activated methyl cycle and formaldehyde detoxification arecoupled using CytoSolve to produce an integrative model of C1 metabolism. The earlier results in Sections 3.2, 3.3 and 3.4 are based on simulations of individual models. The results in this section are from simulations executed on the integrative C1 metabolism model. In the integrated model, the interconnections between individual models can provide insights into how the biomolecular species in one individual model affect the biomolecular species in the other individual model. As before, the simulation time period is maintained at 800,000 seconds (~9 days).

There are three important results that emerge from this integrative simulation: 1) formaldehyde is detoxified completely in C1 metabolism (Section 3.5.1), 2) sarcosine is completely depleted in C1 metabolism (Section 3.5.2), and 3) glutathione is maintained at steady state levels in C1 metabolism (Section 3.5.3).

3.4.1. Formaldehyde Is Detoxified in C1 Metabolism

First result is, as shown in **Figure 12**, formaldehyde concentration is completely eliminated during C1 metabolism. This result is consistent with the results obtained for the individual formaldehyde detoxification model in **Figure 10**. The integrative model of C1 metabolism, unlike the individual model of formaldehyde detoxification, reveals that the initial quantity of formaldehyde is higher. This variation is likely due to the fact that there are more sources of formaldehyde synthesis in the C1 metabolism model compared to the individual formaldehyde detoxification model.

One other variation is that the clearance time for formaldehyde appears to be ~200,000 seconds (~2 days) in the integrative model versus ~120,000 (~1.5 days) in the individual formaldehyde detoxification model. This is again likely due to the higher amount of initial formaldehyde present.

3.4.2. Sarcosine Is Depleted in C1 Metabolism

The second result is, as shown in **Figure 13**, sarcosine concentrations decrease with time and reach zero. This result differs from the results obtained for the individual activated methyl cycle model in **Figure 9**. This variation is likely due to the complete conversion of sarcosine in the integrative C1 metabolism model, which canoccur since sarcosine, unlike in the individual activated methyl cycle model, is utilized for synthesis of formaldehyde. In the individual activated methyl cycle model, there are no reactions that force the consumption of sarcosine.
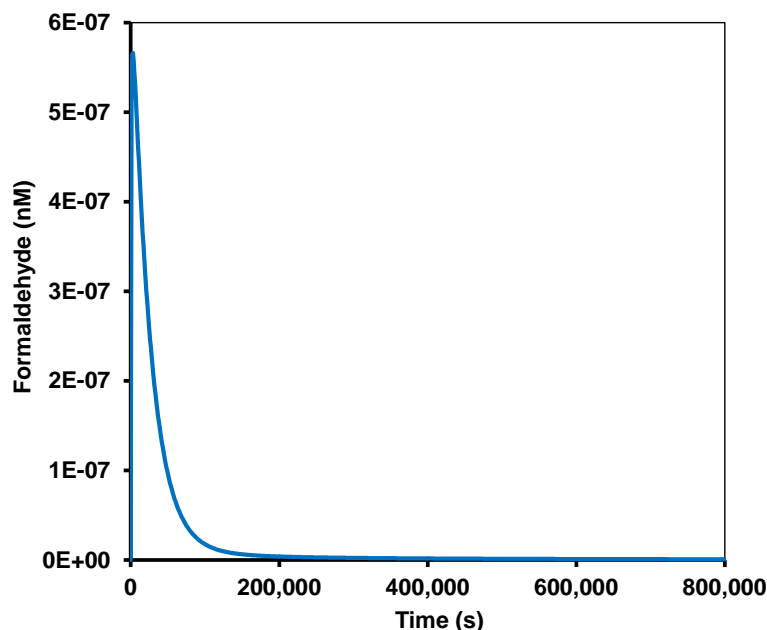
Figure 12. Simulation results of formaldehyde concentration from integrative C1 metabolism model.
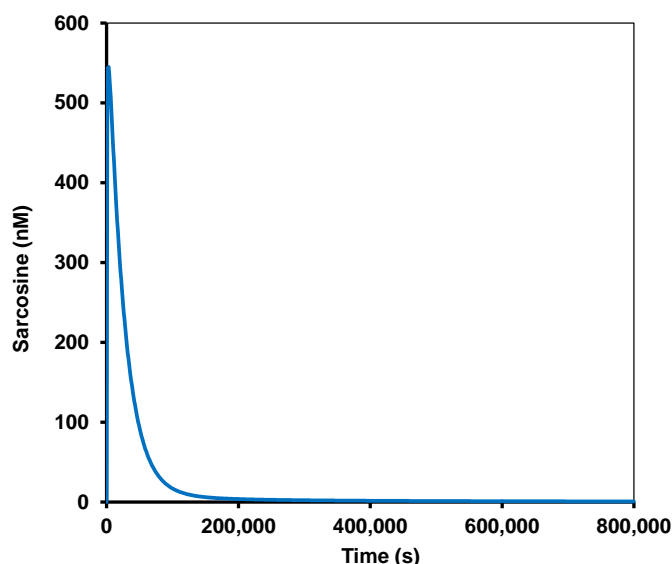
Figure 13. Simulation results of sarcosine concentration from integrative C1 metabolism model.

3.4.3. Glutathione Is Maintained at Steady State Levels in C1 Metabolism

The third result is, as shown in **Figure 14**, glutathione concentrations are maintained at a steady state level of 5,000,000 nM. This result is the same as in the individual formaldehyde detoxification model shown in **Figure 11**. This consistent steady state value between individual formaldehyde detoxification model and integrative C1 metabolism model is likely because there is minimal consumption of glutathione (GSH) in the integrative model of C1 metabolism as well as in the formaldehyde detoxification model. Moreover, any glutathione that is consumed is likely recycled back from the GSH-formaldehyde adduct, which is hydrolyzed by for mylglutathione hydrolase [28], thus maintaining a consistent steady state level.

3.5. Parameter Sensitivity Analysis on C1 Metabolism Model

The results from the *in silico* modeling of C1 metabolism have provided insights on key biomolecular species, such as formaldehyde, formate, sarcosine and glutathione. These simulation results are highly dependent on the integrity of the literature reviewed and in particular on the kinetic rate constants used in the modeling. Parameter sensitivity analysis provides a method to appreciate the relative significance of critical parameters.

Given the importance of formaldehyde synthesis and clearance in C1 metabolism, parameter sensitivity analysis was performed on the following three critical parameters:

1. kFTD—Rate constant for conversion of 5,10-methylene-THF to formaldehyde;
2. VCAT—Rate of formaldehyde production from methanol;
3. kGSH-HCHO—Binding rate constant of glutathione (GSH) and formaldehyde (HCHO).

Three sets of results emerge from the sensitivity analysis. First, kFTD, is varied from 1.4 to 5.6 s^{-1} and the resulting formaldehyde concentrations are simulated and observed for the integrated model of C1 metabolism in **Figure 15**. The results indicate that, formaldehyde concentrations are not sensitive to kFTD in the integrative C1 metabolism model.

VCAT is varied from 22 to 100 nM/s, and the resulting formaldehyde concentrations are simulated and observed for the integrated model of C1 metabolism in **Figure 16**. The results indicate that, formaldehyde concentrations are not sensitive to VCAT in the integrative C1 metabolism model.

Third, kGSH-HCHO is varied from 0.000864 to 0.00864 $nM^{-1} \cdot s^{-1}$, and the resulting formaldehyde concentrations are simulated and observed for the integrated model of C1 metabolism in **Figure 17**. The results indicate that, as kGSH-HCHO is increased, the formaldehyde concentration is decreased over time. Therefore, from a parameter sensitivity standpoint, unlike kFTD and VCAT, formaldehyde concentrations are highly sensitive to variations in kGSH-HCHO in the integrative C1 metabolism model. Although the parameter value varies across one order of magnitude, formaldehyde is completely detoxified in all cases.
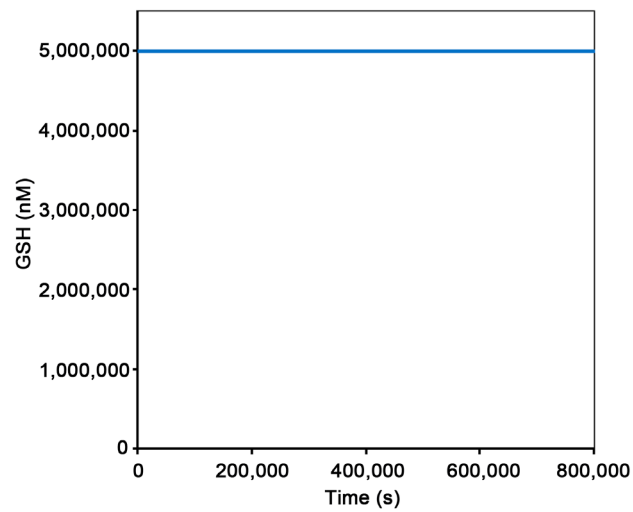
Figure 14. Simulation results of glutathione (GSH) concentration from integrative C1 metabolism model.
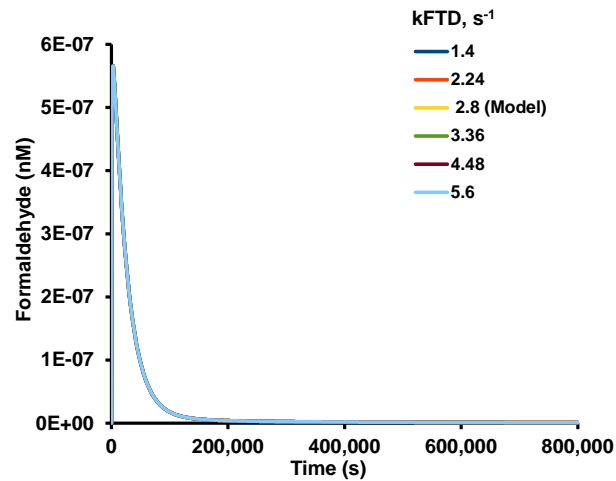
Figure 15. Parameter sensitivity analysis of kFTD in the C1 metabolism model.
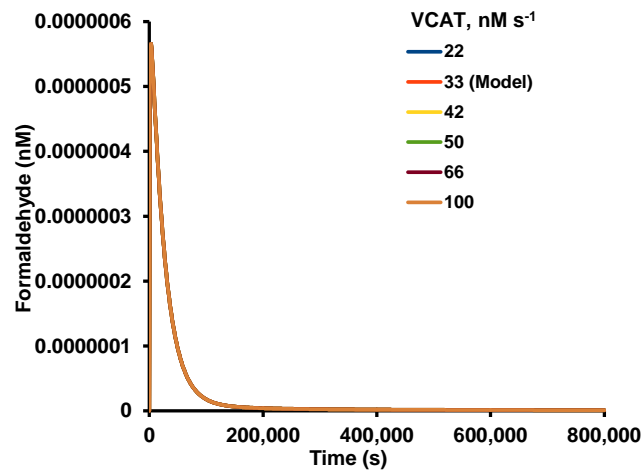
Figure 16. Formaldehyde concentration simulation results for integrated C1 metabolism model.

Figure 17. Formaldehyde concentration simulation results for integrated C1 metabolism model.

4. Discussion and Conclusions

This work provides, to the authors' knowledge, the first *in silico*, predictive and computational model of C1 metabolism. A global systems architecture map was developed, from an earlier systematic review, to provide a high-level understanding of the interrelationships of the three molecular systems of C1 metabolism: methionine biosynthesis, activated methyl cycle and formaldehyde detoxif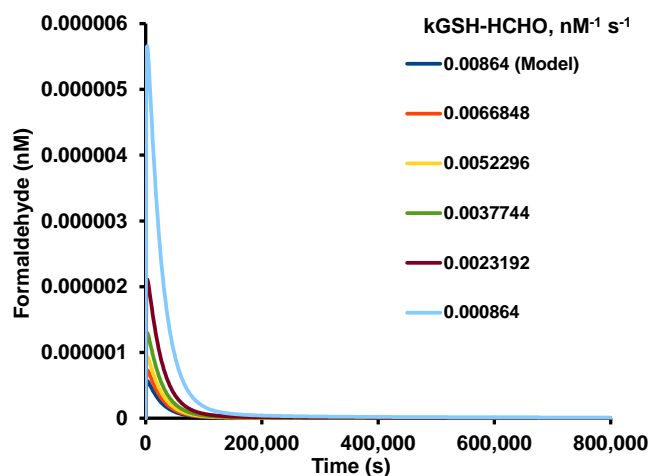ication. In addition, another systems architecture map was also developed to provide understanding of related molecular systems that may affect and be affected by C1 metabolism.

The systems architecture was then used within the CytoSolve Collaboratory to integrate the three molecular systems of C1 metabolism to produce an integrative model. Simulations were executed on the individual models as well as the integrative C1 metabolism model. The individual models predict temporal behavior of key biomolecules in C1 metabolism such as formaldehyde, formate, sarcosine and glutathione. The integrative C1 metabolism model provides new insights and predictions of formaldehyde, sarcosine and glutathione, and affords a vehicle for hypothesis testing difficult to perform *in vitro* and *in vivo*.

The integrative model of C1 metabolism predicts that in normal plants, formaldehyde is evanescently produced and detoxified rapidly between ~1.5 and ~2 days. Glutathione levels are minimally affected and maintain a steady state of 5,000,000 nM. Finally, sarcosine is fully consumed during C1 metabolism.

Parameter sensitivity analysis reveals that variations in kGSH-HCHO, binding rate constant of glutathione (GSH) and formaldehyde (HCHO), affect formaldehyde concentration in normal plants. Even an order of magnitude variation in this parameter, however, still results in complete formaldehyde detoxification. In summary, formaldehyde is fully detoxified, though with some temporal variations, regardless of the values of kGSH-HCHO tested.

5. Future Directions

The systems architecture map in **Figure 7** provides a blueprint for further research on the integrative model of C1 metabolism model discussed herein. Clearly, there are many other neighboring biological processes that interact with C1 metabolism, such as THF biosynthesis, oxidative stress metabolism, catalase activity, shikimic acid metabolism, adenosine metabolism, glyphosate metabolism, formate biosynthesis, and serine biosynthesis, for example.

The *in silico* model of C1 metabolism, now resident in the CytoSolve Collaboratory, offers a scalable and transparent research platform not only to study C1 metabolism, but also to expand and explore how other molecular systems may affect and be affected by C1 metabolism. The authors believe that oxidative stress, for example, is one such important molecular system that, in the near term, should be investigated, modeled and integrated within the C1 metabolism model. Empirical data have suggested that oxidative stress may have some significant effects on species such as formaldehyde and glutathione. However, such exploration is difficult through

current *in vivo* and *in vitro* approaches. The systems architecture of C1 metabolism may, however, now provide an efficient *in silico* mechanism to explore the molecular systems integration problem of oxidative stress systems with C1 metabolism to understand the effects of oxidative stress on formaldehyde and glutathione levels.

The mathematical models developed in this study are based on the known literature reviewed by the authors. Giving scientific publishing is a dynamic process, and the CytoSolve Collaboratory provides a method to incorporate any new, updated and missing literature to enhance the model in a transparent and collaborative manner. This means that the C1 metabolism model shared in this research can be constantly updated to maintain its relevancy and usefulness based on new information. The approach presented herein, beyond expansion and understanding of C1 metabolism, may likely provide a new paradigm for scientific research through systems biology approaches, where transparency and collaboration, accessible in a computational research framework, become a critical element of scientific inquiry.

References

[1] Hanson, A.D., Gage, D.A. and Shachar-Hill, Y. (2000) Plant One-Carbon Metabolism and Its Engineering. *Trends in Plant Science*, **5**, 206-213. http://dx.doi.org/10.1016/S1360-1385(00)01599-5

[2] Hanson, A.D. and Roje, S. (2001) One-Carbon Metabolism in Higher Plants. *Annual Review of Plant Physiology and Plant Molecular Biology*, **52**, 119-137. http://dx.doi.org/10.1146/annurev.arplant.52.1.119

[3] Vanyushin, B.F. (2006) DNA Methylation in Plants: DNA Methylation: Basic Mechanisms. Springer, Berlin, Heidelberg.

[4] Deonikar, P., Kothandaram, S., Mohan, M., Kollin, C., Konecky, P., Olovyanniko, R., Zamore, Z., Carey, B. and Ayyadurai, V.A.S. (2015) Discovery of Key Molecular Pathways of C1 Metabolism and Formaldehyde Detoxification in Maize through a Systematic Bioinformatics Literature Review. *Agricultural Sciences*, **6**, 571-585. http://dx.doi.org/10.4236/as.2015.65056

[5] Ayyadurai, V.A.S. and Dewey, C.F. (2011) CytoSolve: A Methodology for Dynamic Integration of Multiple Molecular Pathway Models. *Cellular and Molecular Bioengineering*, **4**, 28-45. http://dx.doi.org/10.1007/s12195-010-0143-x

[6] Ayyadurai, V.A.S. (2011) Services-Based Systems Architecture for Modeling the Whole Cell: A Distributed Collaborative Engineering Systems Approach. *Communications in Medical and Care Compunetics*, **1**, 115-168.

[7] Mouillon, J.M., Aubert, S., Bourguignon, J., Gout, E., Douce, R. and Rébeillé, F. (1999) Glycine and Serine Catabolism in Non-Photosynthetic Higher Plant Cells: Their Role in C1 Metabolism. *The Plant Journal*, **20**, 197-205. http://dx.doi.org/10.1046/j.1365-313x.1999.00591.x

[8] Peacock, D. and Boulter, D. (1970) Kinetic Studies of Formate Dehydrogenase. *Biochemical Journal*, **120**, 763-769.

[9] Zhang, W., Tang, L., Sun, H., *et al.* (2014) C1 Metabolism Plays an Important Role during Formaldehyde Metabolism and Detoxification in Petunia Under Liquid HCHO Stress. *Plant Physiology and Biochemistry*, **83**, 327-336. http://dx.doi.org/10.1016/j.plaphy.2014.08.017

[10] Janave, M.T., Ramaswamy, N.K. and Nair, P.M. (1993) Purification and Characterization of Glyoxylatesynthetase from Greening Potato-Tuber Chloroplasts. *European Journal of Biochemistry*, **214**, 889-896. http://dx.doi.org/10.1111/j.1432-1033.1993.tb17992.x

[11] Ravanel, S., Block, M.A., Rippert, P., *et al.* (2004) Methionine Metabolism in Plants: Chloroplasts Are Autonomous for *de Novo* Methionine Synthesis and Can Import S-Adenosylmethionine from the Cytosol. *The Journal of Biological Chemistry*, **279**, 22548-22557. http://dx.doi.org/10.1074/jbc.M313250200

[12] Chen, L., Chan, S.Y. and Cossins, E.A. (1997) Distribution of Folate Derivatives and Enzymes for Synthesis of 10-Formyltetrahydrofolate in Cytosolic and Mitochondrial Fractions of Pea Leaves. *Plant Physiology*, **115**, 299-309.

[13] Hanson, A.D. and Gregory, J.F. (2011) Folate Biosynthesis, Turnover, and Transport in Plants. *Annual Review of Plant Biology*, **62**, 105-125. http://dx.doi.org/10.1146/annurev-arplant-042110-103819

[14] Rébeillé, F., Stephane, R., Jabrin, S., Douce, R., Storozhenko, S., Re, F. and Van Der Straeten, D. (2006) Folates in Plants: Biosynthesis, Distribution, and Enhancement. *Physiologia Plantarum*, **126**, 330-342. http://dx.doi.org/10.1111/j.1399-3054.2006.00587.x

[15] Appling, D.R. (1991) Compartmentation of Folate-Mediated One-Carbon Metabolism in Eukaryotes. *The FASEB Journal*, **5**, 2645-2651.

[16] Neuburger, M., Rébeillé, F., Jourdain, A., Nakamura, S. and Douce, R. (1996) Mitochondria Are a Major Site for Folate and Thymidylate Synthesis in Plants. *The Journal of Biological Chemistry*, **271**, 9466-9472. http://dx.doi.org/10.1074/jbc.271.16.9466

[17] Sahr, T., Ravanel, S. and Rébeillé, F. (2005) Tetrahydrofolate Biosynthesis and Distribution in Higher Plants. *Bio-

chemical Society Transactions, **33**, 758-762.

[18] Rebeille, F., Neuburger, M. and Douce, R. (1994) Interaction between Glycine Decarboxylase, Serine Hydroxymethyltransferase and Tetrahydrofolate Polyglutamates in Pea Leaf Mitochondria. *Biochemical Journal*, **302**, 223-228.

[19] Kim, D.G., Park, T.J., Kim, J.Y. and Cho, Y.D. (1995) Purification and Characterization of S-Adenosylmethionine Synthetase from Soybean (*Glycine max*) Axes. *Journal of Biochemistry and Molecular Biology*, **28**, 100-106.

[20] Ravanel, S., Gakière, B., Job, D. and Douce, R. (1998) The Specific Features of Methionine Biosynthesis and Metabolism in Plants. *Proceedings of the National Academy of Sciences of the United States of America*, **95**, 7805-7812. http://dx.doi.org/10.1073/pnas.95.13.7805

[21] Ravanel, S., Gambonnet, B., Douce, R. and Rébeillé, F. (2003) One-Carbon Metabolism in Plants. Regulation of Tetrahydrofolate Synthesis during Germination and Seedling Development. *Plant Physiology*, **131**, 1431-1439. http://dx.doi.org/10.1104/pp.016915

[22] James, F., Nolte, K.D. and Hanson, A.D. (1995) Purification and Properties of *S*-Adenosyl-L-methionine: L-Methionine *S*-Methyltransferase from *Wollastonia biflora* Leaves. *The Journal of Biological Chemistry*, **270**, 22344-22350. http://dx.doi.org/10.1074/jbc.270.38.22344

[23] Bradbury, L.M.T., Ziemak, M.J., El Badawi-Sidhu, M., Fiehn, O. and Hanson, A.D. (2014) Plant-Driven Repurposing of the Ancient S-Adenosylmethionine Repair Enzyme Homocysteine S-Methyltransferase. *Biochemical Journal*, **463**, 279-286.

[24] Achkor, H., Díaz, M., Fernández, M.R., Biosca, J.A., Parés, X. and Martínez, M.C. (2003) Enhanced Formaldehyde Detoxification by Overexpression of Glutathione-Dependent Formaldehyde Dehydrogenase from Arabidopsis. *Plant Physiology*, **132**, 2248-2255. http://dx.doi.org/10.1104/pp.103.022277

[25] Goyer, A., Johnson, T.L., Olsen, L.J., Collakova, E., Shachar-Hill, Y., Rhodes, D. and Hanson, A.D. (2004) Characterization and Metabolic Function of a Peroxisomalsarcosine and Pipecolate Oxidase from Arabidopsis. *The Journal of Biological Chemistry*, **279**, 16947-16953. http://dx.doi.org/10.1074/jbc.M400071200

[26] Li, R., Moore, M. and King, J. (2003) Investigating the Regulation of One-Carbon Metabolism in *Arabidopsis thaliana*. *Plant and Cell Physiology*, **44**, 233-241. http://dx.doi.org/10.1093/pcp/pcg029

[27] Vivancos, P.D., Driscoll, S.P., Bulman, C., Ying, L., Emami, K., Treumann, A., Mauve, C., Noctor, G. and Foyer, C.H. (2011) Perturbations of Amino Acid Metabolism Associated with Glyphosate-Dependent Inhibition of Shikimic Acid Metabolism Affect Cellular Redox Homeostasis and Alter the Abundance of Proteins Involved in Photosynthesis and Photorespiration. *Plant Physiology*, **157**, 256-268. http://dx.doi.org/10.1104/pp.111.181024

[28] Díaz, M., Achkor, H., Titarenko, E. and Martínez, M.C. (2003) The Gene Encoding Glutathione-Dependent Formaldehyde Dehydrogenase/GSNO Reductase Is Responsive to Wounding, Jasmonic Acid and Salicylic Acid. *FEBS Letters*, **543**, 136-139. http://dx.doi.org/10.1016/S0014-5793(03)00426-5

[29] Kordic, S., Cummins, I. and Edwards, R. (2002) Cloning and Characterization of an S-Formylglutathione Hydrolase from *Arabidopsis thaliana*. *Archives of Biochemistry and Biophysics*, **399**, 232-238. http://dx.doi.org/10.1006/abbi.2002.2772

[30] Martinez, M.C., Achkor, H., Perssonz, B., Fernandez, M.R., Shafqat, J. and Farres, J. (1996) Arabidopsis Formaldehyde Dehydrogenase Molecular Properties of Plant Class III Alcohol Dehydrogenase Provide Further Insights into the Origins, Structure and Function of Plant Class P and Liver Class I Alcohol Dehydrogenases. *European Journal of Biochemistry*, **241**, 849-857. http://dx.doi.org/10.1111/j.1432-1033.1996.00849.x

[31] Wippermann, U., Fliegmann, J., Bauw, G., Langebartels, C., Maier, K. and Sandermann, H. (1999) Maize Glutathione-Dependent Formaldehyde Dehydrogenase: Protein Sequence and Catalytic Properties. *Planta*, **208**, 12-18. http://dx.doi.org/10.1007/s004250050529

[32] Koo, A., Nordsletten, D., Umeton, R., Yankama, B., Ayyadurai, S., García-Cardeña, G. and Dewey Jr., C.F. (2013) In Silico Modeling of Shear-Stress-Induced Nitric Oxide Production in Endothelial Cells through Systems Biology. *Biophysical Journal*, **104**, 2295-2306. http://dx.doi.org/10.1016/j.bpj.2013.03.052

[33] Nijhout, H.F., Reed, M.C., Budu, P. and Ulrich, C.M. (2004) A Mathematical Model of the Folate Cycle: New Insights into Folate Homeostasis. *The Journal of Biological Chemistry*, **279**, 55008-55016. http://dx.doi.org/10.1074/jbc.M410818200

[34] Zhang, Y., Sun, K., Sandoval, F.J., Santiago, K. and Roje, S. (2010) One-Carbon Metabolism in Plants: Characterization of a Plastid Serine Hydroxymethyltransferase. *Biochemical Journal*, **430**, 97-105.

[35] Yokota, A., Kitaoka, S., Miura, K. and Wadano, A. (1985) Reactivity of Glyoxylate with Hydrogen Perioxide and Simulation of the Glycolate Pathway of C3 Plants and Euglena. *Planta*, **165**, 59-67. http://dx.doi.org/10.1007/BF00392212

[36] Yeo, E. and Wagner, C. (1992) Purification and Properties of Pancreatic Glycine N-Methyltransferase. *The Journal of Biological Chemistry*, **267**, 24669-24674.

[37] Ogawa, H., Gomi, T. and Fujioka, M. (1993) Mammalian Glycine N-Methyltransferases. Comparative Kinetic and Structural Properties of the Enzymes from Human, Rat, Rabbit and Pig Livers. *Comparative Biochemistry and Physiology-Part B*, *Biochemistry*, **106**, 601-611.

[38] Alekseeva, A.A., Savin, S.S. and Tishkov, V.I. (2011) NAD$^+$-Dependent Formate Dehydrogenase from Plants. *Acta Naturae*, **3**, 38-54.

[39] Kallen, R.G. and Jencks, P. (1966) The Mechanism of the Condensation of Formaldehyde with Tetrahydrofolic Acid. *The Journal of Biological Chemistry*, **241**, 5851-5863.

[40] Havir, E.A. and McHale, N.A. (1989) Enhanced-Peroxidatic Activity in Specific Catalase Isozymes of Tobacco, Barley, and Maize. *Plant Physiology*, **91**, 812-815. http://dx.doi.org/10.1104/pp.91.3.812

[41] Wlodek, L. (1988) The Reaction of Sulfhydryl Groups with Carbonyl Compounds. *Acta Biochimica Polonica*, **35**, 307-317.

[42] Wippermann, U., Fliegmann, J., Bauw, G., Langebartels, C., Maier, K. and Sandermann, H. (1999) Maize Glutathione-Dependent Formaldehyde Dehydrogenase: Protein Sequence and Catalytic Properties. *Planta*, **208**, 12-18. http://dx.doi.org/10.1007/s004250050529

Supplementary Materials

Table S1. List of parameters used in *in silico* models of methionine biosynthesis.

Kinetic Parameter	Description	Reference
KAICAR	Michaelis Menten constant of AICAR transformylase converting AICAR to FAICAR	[S1]
kDHFR	Rate constant of dihydrofolate reductase converting DHF to THF	[S2]
KDHFR	Michaelis Menten constant for dihydrofolate reductase converting DHF to THF	[S2]
KFTCD	Michaelis Menten constant for 5-formimino-THF cyclodeaminase converting 5-formimino-THF to 5,10-methenyl-THF	[S3]
kFTCL	Rate constant of 5-formyl THF cycloligase converting 5-formyl THF to 5,10-methenyl THF	[S4]
KFTS	Michaelis Menten constant for formyl-THF synthetase converting formate to 10-formyl-THF	[S5]
KGDC	Michaelis Menten constant for glycine decarboxylase converting THF to 5,10-methylene THF	[S6]
kGF	Second order conversion rate of glyoxylate to formate	[S7]
KGFT	Michaelis Menten constant for glutamate formiminotransferase converting formiminoglutamate to 5-formimino-THF	[S8]
KGSYN	Michaelis Menten constant for glyoxylate synthetase converting formate to glyoxylate	[S9]
KGTF	Michaelis Menten constant for GAR transformylase converting GAR to FGAR	[S10]
KKHMT	Michaelis Menten constant for ketopantoate hydroxymethyltransferase converting a-KIVA to THF and ketopantoate	[S11]
kMHF_GAR	Rate constant for GAR transformylase converting 10-formyl-THF to THF	[S10]
KMTC	Michaelis Menten constant for 5,10-methylene THF cyclohydrolase converting 5,10-methenyl-THF to 10-formyl-THF	[S12]
KMTD	Michaelis Menten constant for 5,10-methylene THF dehydrogenase converting 5,10-methylene-THF to 5,10-methenyl-THF	[S12]
kMTR	Rate constant for methylene THF reductase converting 5,10-methylene-THF to 5-methyl-THF	[S13]
KMTR	Michaelis Menten constant for methylene THF reductase converting 5,10-methylene-THF to 5-methyl-THF	[S13]
KMTS	Michaelis Menten constant for methionine synthase converting homocysteine to methionine	[S14]
kSHM	Rate constant for serine hydroxymethyltransferase converting 5,10-methenyl-THF to 5-formyl-THF	[S15]
KSHM	Michaelis Menten constant for serine hydroxymethyl transferase converting 5,10-methenyl-THF to 5-formyl-THF	[S15]
kSHMT	Rate constant for serine hydroxymethyltransferase converting serine to glycine	[S16]
KSHMT	Michaelis Menten constant for serine hydroxymethyltransferase converting serine to glycine	[S16]
kTFA	Rate constant for the association of THF and Formaldehyde to 5,10-methylene-THF	[S17]
kTFD	Rate constant for the dissociation of 5,10-methylene-THF to THF and Formaldehyde	[S17]
KTS	Michaelis Menten for thymidylate synthase induced synthesis of thymidylate from 5,10-methenyl-THF	[S18]
VAICAR	Vmax of AICAR transformylase converting AICAR to FAICAR	[S1]
VFTCD	Vmax for 5-formimino-THF cyclodeaminase converting 5-formimino-THF to 5,10-methenyl-THF	[S3]
VFTS	Vmax for formyl-THF synthetase converting formate to 10-formyl-THF	[S5]
VGDC	Vmax for glycine decarboxylase converting THF to 5,10-methylene THF	[S6]
VGFT	Vmax for glutamate formiminotransferase converting formiminoglutamate to 5-formimino-THF	[S8]
VGSYN	Vmax for glyoxylate synthetase converting formate to glyoxylate	[S9]
VGTF	Vmax for GAR transformylase converting GAR to FGAR	[S10]
VKHMT	Vmax for ketopantoate hydroxymethyltransferase converting a-KIVA to THF and ketopantoate	[S34]

Table S2. List of parameters used in *in silico* model of activated methyl cycle.

Kinetic Parameter	Description	Reference
KSAM	Michaelis Menten constant for s-adenosyl methionine synthase converting methionine to SAM	[S19]
VSAM	Vmax for s-adenosyl methionine synthase converting methionine to SAM	[S19]
VMTG	Vmax for glycine methyltransferase converting glycine to sarcosine	[S20]
KMTA	Michaelis Menten constant for glycine methyltransferase converting SAM to SAH	[S21]
KMTG	Michaelis Menten constant for glycine methyltransferase converting glycine to sarcosine	[S21]
KSAH	Michaelis Menten constant for the dissociation of SAH to adenosine and homocysteine induced by s-adenosyl homocysteine hydrolase	[S22]
VSAH	Vmax for the dissociation of SAH to adenosine and homocysteine induced by s-adenosyl homocysteine hydrolase	[S22]
kHMT	Rate constant for the association of SMM and homocysteine to methionine induced by homocysteine methyltransferase	[S23]
KHMT	Michaelis Menten constant for the association of SMM and homocysteine to methionine induced by homocysteine methyltransferase	[S23]
KMMT	Michaelis Menten constant for Methionine methyltransferase converting Methionine to SMM	[S24]
VMMT	Vmax for methionine methyltransferase converting methionine to SMM	[S24]
VADOK	Vmax for adenosine kinase converting adenosine to AMP	[S25]
KADOK	Michaelis Menten constant for adenosine kinase converting adenosine to AMP	[S25]
VADEK	Vmax for adenylate kinase converting ADP to AMP and ATP	[S26]
KADEK	Michaelis Menten constant for adenylate kinase converting ADP to AMP and ATP	[S26]
KSAM	Michaelis Menten constant for S-adenosyl methionine synthase converting methionine to SAM	[S19]
VSAM	Vmax for S-adenosyl methionine synthase converting methionine to SAM	[S19]
VMTG	Vmax for Glycine methyltransferase converting glycine to sarcosine	[S20]
KMTA	Michaelis Menten constant for glycine methyltransferase converting SAM to SAH	[S21]
KMTG	Michaelis Menten constant for glycine methyltransferase converting glycine to sarcosine	[S21]
KSAH	Michaelis Menten constant for the dissociation of SAH to adenosine and homocysteine induced by s-adenosyl homocysteine hydrolase	[S22]
VSAH	Vmax for the dissociation of SAH to adenosine and homocysteine induced by s-adenosyl homocysteine hydrolase	[S22]
kHMT	Rate constant for the association of SMM and homocysteine to methionine induced by homocysteine methyltransferase	[S23]
KHMT	Michaelis Menten constant for the association of SMM and homocysteine to methionine induced by homocysteine methyltransferase	[S23]
KMMT	Michaelis Menten constant for methionine methyltransferase converting methionine to SMM	[S24]

Table S3. List of parameters used in *in silico* model of formaldehyde detoxification.

Kinetic Parameter	Description	Reference
kTFD	Rate constant for the dissociation of 5,10-methylene-THF to THF and formaldehyde	[S17]
kTFA	Rate constant for the association of THF and formaldehyde to 5,10-methylene-THF	[S17]
VCAT	Vmax for catalase converting methanol to formaldehyde	[S27]
KCAT	Michaelis Menten constant for catalase converting cethanol to formaldehyde	[S28]

Continued

kSOX	Rate constant for sarcosine oxidase converting sarcosine to glycine and formaldehyde	[S29]
KSOX	Michaelis Menten constant for sarcosine oxidase converting sarcosine to glycine and formaldehyde	[S29]
kGSHdissF	Rate constant for the dissociation of HM-GSH to GSH and formaldehyde	[S30]
kGSHbindF	Rate constant for the association of GSH and formaldehyde to HM-GSH	[S30]
VFALDH	Vmax for FALDH induced GSH formaldehyde adduct formation	[S31]
KFALDHN	Michaelis Menten constant for FALDH converting NAD to NADH	[S31]
KFALDH	Michaelis Menten constant for FALDH induced GSH formaldehyde adduct formation	[S31]
VFGH	Vmax for FGH converting formyl-GSH to formate	[S32]
KFGH	Michaelis Menten constant for FGH converting formyl-GSH to formate	[S32]
kFDH	Rate constant for FDH induced conversion of formate to H_2O and CO_2	[S33]
KFDH	Michaelis Menten constant for FDH induced conversion of formate to H_2O and CO_2	[S33]
kTFD	Rate constant for the dissociation of 5,10-methylene-THF to THF and formaldehyde	[S17]
kTFA	Rate constant for the association of THF and Formaldehyde to 5,10-methylene-THF	[S17]
VCAT	Vmax for catalase converting methanol to formaldehyde	[S27]
KCAT	Michaelis Menten constant for catalase converting cethanol to formaldehyde	[S28]
kSOX	Rate constant for sarcosine oxidase converting sarcosine to glycine and formaldehyde	[S29]
KSOX	Michaelis Menten constant for sarcosine oxidase converting sarcosine to glycine and formaldehyde	[S29]
kGSHdissF	Rate constant for the dissociation of HM-GSH to GSH and formaldehyde	[S30]
kGSHbindF	Rate constant for the association of GSH and formaldehyde to HM-GSH	[S30]
VFALDH	Vmax for FALDH induced GSH formaldehyde adduct formation	[S31]
KFALDHN	Michaelis Menten constant for FALDH converting NAD to NADH	[S31]

Supplementary Materials References

[S1] Nijhout, H.F., Reed, M.C., Budu, P. and Ulrich, C.M. (2004) A Mathematical Model of the Folate Cycle: New Insights into Folate Homeostasis. *The Journal of Biological Chemistry*, **279**, 55008-55016. http://dx.doi.org/10.1074/jbc.M410818200

[S2] Ratnam, S., Delcamp, T.J., Hynes, J.B. and Freisheim, J.H. (1987) Purification and Characterization of Dihydrofolate Reductase from Soybean Seedlings. *Archives of Biochemistry and Biophysics*, **255**, 279-289. http://dx.doi.org/10.1016/0003-9861(87)90395-X

[S3] Uyeda, K. and Rabisowitz, J.C. (1967) Metabolism of Formiminoglycine- Formiminotetrahydrofolate Cyclodeaminase. *The Journal of Biological Chemistry*, **242**, 24-31.

[S4] Roje, S., Janave, M.T., Ziemak, M.J. and Hanson, A.D. (2002) Cloning and Characterization of Mitochondrial 5-Formyltetrahydrofolate Cycloligase from Higher Plants. *The Journal of Biological Chemistry*, **277**, 42748-42754. http://dx.doi.org/10.1074/jbc.M205632200

[S5] Nour, J.M. and Rabinowitzs, J.C. (1991) Isolation, Characterization, and Structural Organization of 10-Formyltetrahydrofolate Synthetase from Spinach Leaves. *The Journal of Biological Chemistry*, **266**, 18363-18369.

[S6] Besson, V., Rebeille, F., Neuburger, M., Douce, R. and Cossinst, E.A. (1993) Effects of Tetrahydrofolate Polyglutamates on the Kinetic Parameters of serine Hydroxymethyltransferase and Glycine Decarboxylase from Pea Leaf Mitochondria. *Biochemical Journal*, **292**, 425-430.

[S7] Yokota, A., Kitaoka, S., Miura, K. and Wadano, A. (1985) Reactivity of Glyoxylate with Hydrogen Perioxide and Simulation of the Glycolate Pathway of C3 Plants and Euglena. *Planta*, **165**, 59-67. http://dx.doi.org/10.1007/BF00392212

[S8] Bortoluzzi, L.C. and MacKenzie, R.E. (1983) Glutamate Formyl- and Formimino-Transferase Activities from Pig Liver. *Biochemistry and Cell Biology*, **61**, 248-253. http://dx.doi.org/10.1139/o83-035

[S9] Janave, M.T., Ramaswamy, N.K. and Nair, P.M. (1993) Purification and Characterization of Glyoxylatesynthetase from Greening Potato-Tuber Chloroplasts. *European Journal of Biochemistry*, **214**, 889-896. http://dx.doi.org/10.1111/j.1432-1033.1993.tb17992.x

[S10] Caperelli, C.A., Benkovic, P.A., Chettur, G. and Benkovicl, S.J. (1980) Purification of a Complex Catalyzing Folate Cofactor Synthesis and Transformylation in *de Novo* Purine Biosynthesis. *The Journal of Biological Chemistry*, **255**, 1885-1890.

[S11] Powers, S.U.E.G. and Snell, E.E. (1976) Ketopantoate Hydroxymethyltransferase: II. Physical, Catalytic and Regulatory Properties. *The Journal of Biological Chemistry*, **251**, 3786-3793.

[S12] Kirk, C., Chen, L., Imeson, H.C. and Cossins, E.A. (1995) A 5,10-Methylenetetrahydrofolate Dehydrogenase: 5,10-Methylenetetrahydrofolate Cyclohydrolase Protein from *Pisum sativum*. *Phytochemistry*, **39**, 1309-1317. http://dx.doi.org/10.1016/0031-9422(95)97864-6

[S13] Sheppard, C.A., Trimmer, E.E. and Matthews, R.G. (1999) Purification and Properties of NADH-Dependent 5,10-Methylenetetrahydrofolate Reductase (MetF) from *Escherichia coli*. *Journal of Bacteriology*, **181**, 718-725.

[S14] Eichel, J., Gonzhez, J.C., Hotze, M., Matthews, R.G. and Schroder, J. (1995) Vitamin-B12-Independent Methionine Synthase from a Higher Plant. *European Journal of Biochemistry*, **230**, 1053-1058.

[S15] Stover, P. and Schirch, V. (1992) Enzymatic Mechanism for the Hydrolysis of 5,10-Methenyltetrahydropteroylglutamate to 5-Formyltetrahydropteroylglutamate by Serine Hydroxymethyltransferase. *Biochemistry*, **31**, 2155-2164. http://dx.doi.org/10.1021/bi00122a037

[S16] Zhang, Y., Sun, K., Sandoval, F.J., Santiago, K. and Roje, S. (2010) One-Carbon Metabolism in Plants: Characterization of a Plastid Serine Hydroxymethyltransferase. *Biochemical Journal*, **430**, 97-105. http://dx.doi.org/10.1042/bj20100566

[S17] Kallen, R.G. and Jencks, P. (1966) The Mechanism of the Condensation of Formaldehyde with Tetrahydrofolic Acid. *The Journal of Biological Chemistry*, **241**, 5851-5863.

[S18] Nielsen, E. and Cella, R. (1988) Thymidylate Synthase in Plant Cells : Kinetic and Molecular Properties of the Enzyme from *Daucus carota* L. Cell Cultures. *Plant and Cell Physiology*, **29**, 503-508.

[S19] Kim, D.G., Park, T.J., Kim, J.Y. and Cho, Y.D. (1995) Purification and Characterization of S-Adenosylmethionine Synthetase from Soybean (*Glycine max*) Axes. *Journal of Biochemistry and Molecular Biology*, **28**, 100-106.

[S20] Yeo, E. and Wagner, C. (1992) Purification and Properties of Pancreatic Glycine N-Methyltransferase. *The Journal of Biological Chemistry*, **267**, 24669-24674.

[S21] Ogawa, H., Gomi, T. and Fujioka, M. (1993) Mammalian Glycine N-Methyltransferases. Comparative Kinetic and Structural Properties of the Enzymes from Human, Rat, Rabbit and Pig Livers. *Comparative Biochemistry and Physiology-Part B*, *Biochemistry*, **106**, 601-611.

[S22] Guranowski, A. and Pawelkiewicz, J. (1977) Adenosylhomocysteinase from Yellow Lupin Seeds. *European Journal of Biochemistry*, **80**, 517-523. http://dx.doi.org/10.1111/j.1432-1033.1977.tb11907.x

[S23] Lyi, S.M., Zhou, X., Kochian, L.V. and Li, L. (2007) Biochemical and Molecular Characterization of the Homocysteine S-Methyltransferase from Broccoli (*Brassica oleracea* var. *italica*). *Phytochemistry*, **68**, 1112-1119. http://dx.doi.org/10.1016/j.phytochem.2007.02.007

[S24] James, F., Nolte, K.D. and Hanson, A.D. (1995) Purification and Properties of *S*-Adenosyl-L-methionine: L-Methionine *S*-Methyltransferase from *Wollastonia biflora* Leaves. *The Journal of Biological Chemistry*, **270**, 22344-22350. http://dx.doi.org/10.1074/jbc.270.38.22344

[S25] Moffatt, B.A., Wang, L., Allen, M.S., Stevens, Y.Y., Qin, W., Snider, J. and Von Schwartzenberg, K. (2000) Adenosine Kinase of Arabidopsis. Kinetic Properties and Gene Expression. *Plant Physiology*, **124**, 1775-1785. http://dx.doi.org/10.1104/pp.124.4.1775

[S26] Murakami, S. and Strotmann, H. (1978) Adenylate Kinase Bound to the Envelope Membranes of Spinach Chloroplasts. *Archives of Biochemistry and Biophysics*, **185**, 30-38. http://dx.doi.org/10.1016/0003-9861(78)90140-6

[S27] Havir, E. A. and McHale, N.A. (1989) Enhanced-Peroxidatic Activity in Specific Catalase Isozymes of Tobacco, Barley, and Maize. *Plant Physiology*, **91**, 812-815. http://dx.doi.org/10.1104/pp.91.3.812

[S28] Havir, E.A. and McHale, N.A. (1990) Purification and Characterization of an Isozyme of Catalase with Enhanced-Peroxidatic Activity from Leaves of *Nicotiana sylvestris*. *Archives of Biochemistry and Biophysics*, **283**, 491-495. http://dx.doi.org/10.1016/0003-9861(90)90672-L

[S29] Goyer, A., Johnson, T.L., Olsen, L.J., Collakova, E., Shachar-Hill, Y., Rhodes, D. and Hanson, A.D. (2004) Characterization and Metabolic Function of a Peroxisomalsarcosine and Pipecolate Oxidase from Arabidopsis. *The Journal of Biological Chemistry*, **279**, 16947-16953. http://dx.doi.org/10.1074/jbc.M400071200

[S30] Wlodek, L. (1988) The Reaction of Sulfhydryl Groups with Carbonyl Compounds. *Acta Biochimica Polonica*, **35**, 307-

317.

[S31] Wippermann, U., Fliegmann, J., Bauw, G., Langebartels, C., Maier, K. and Sandermann, H. (1999) Maize Gluta-thione-Dependent Formaldehyde Dehydrogenase: Protein Sequence and Catalytic Properties. *Planta*, **208**, 12-18.
http://dx.doi.org/10.1007/s004250050529

[S32] Kordic, S., Cummins, I. and Edwards, R. (2002) Cloning and Characterization of an S-Formylglutathione Hydrolase from *Arabidopsis thaliana*. *Archives of Biochemistry and Biophysics*, **399**, 232-238.
http://dx.doi.org/10.1006/abbi.2002.2772

[S33] Alekseeva, A.A., Savin, S.S. and Tishkov, V.I. (2011) NAD$^+$-Dependent Formate Dehydrogenase from Plants. *Acta Naturae*, **3**, 38-54.

[S34] Ottenhof, H.H., Ashurst, J.L., Whitney, H.M., Saldanha, S.A., Schmitzberger, F., Gweon, H.S., Blundell, T.L., Abell, C. and Smith, A.G. (2004) Organisation of the Pantothenate (Vitamin B$_5$) Biosynthesis Pathway in Higher Plants. *The Plant Journal*, **37**, 61-72. http://dx.doi.org/10.1046/j.1365-313X.2003.01940.x